NEW METHODOLOGY TO STUDY THE BEHAVIOUR OF DELAMINATED COMPOSITE STRUCTURES

J.C. Walrick[1], D. Coutellier[2], P. Geoffroy[1], D. Dormegnie[1]

[1]O.N.E.R.A.-I.M.F.L., 5 Boulevard Paul-Painlevé, 59045 Lille Cedex.
[2]L.A.M.I.H-G.M, UMR CNRS 8530, Université de Valenciennes et du Hainaut Cambrésis, BP311 59304 Valenciennes Cedex.

SUMMARY: Laminated composite structures are used in many fields, for example ground transportation. To predict their mechanical behaviour under loading, it is necessary to have a suitable understanding of all the damaging processes such as delamination propagation.
This study intends to detect and follow the delamination growth in a single multi-layer element for a modelling structure in finite elements code. Secondly, we are interested by progressive restitution of delamination effects in laminated modelling structure. The approach is applied with $[90_2/0_2]_s$ plates in three-point bending.
Detection of discontinuous delamination growth front in transverse strips shape is validated by experimental tests. A similar validation is made for delamination effects restitution by comparison with energetic strain levels reached by loaded structure.

KEYWORDS: Delamination, fracture mechanics, behaviour law, modelisation, finite elements, Tsai-Hill criterion, energy density criterion, interface.

CONTEXT FOR THE DELAMINATION STUDY

Numerous studies about delamination growth use fracture mechanics. Most finite element models are made with several shells in the thickness with particular attention to reproduce the stacking sequence [1].
Thus, our approach is different because the set of layers are included in only one single multi-layered shell element Fig. 1.

Therefore, the purpose of this work is to characterize delamination within this single shell. In this case, for the location of delamination, we define an epoxy interface within the laminate, between composite plies [2]. The interface is thinner than the other plies.
However, this element does not allow physical any representation of crack opening displacements (Mode I, in fracture mechanics) associated with delamination. The stress tensor cannot characterize this kind of delamination process within a shell. So, this paper deals only with shear modes II and III, whose associated stress components are already available. Three-point bending was chosen for this study. The plies are glass E/epoxy with 55% volume fibre ratio. The main advantage of bending tests on $[90_2/0_2]_s$ is their simplicity in modelling; moreover the fracture mechanics leading to delamination process are well known and easy to separate from each other [3].

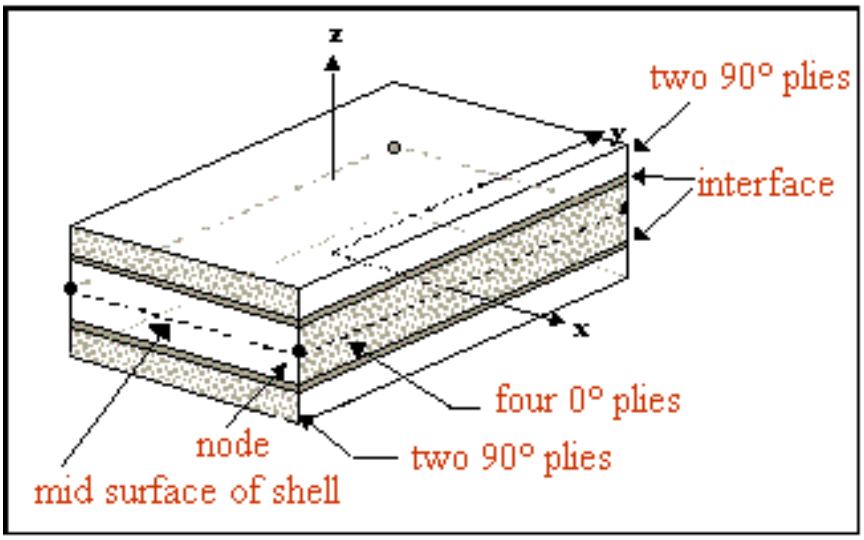

Fig. 1: Type shell multi-layered used for laminated plates $[90_2/0_2]_s$.

MODEL USED

As we have previously seen, the numerical model is based on single multi-layer Mindlin-Reissner shell elements in an explicit computation code. Composite plies produce unidirectional long fibres sequence. The ply model is defined as a homogenous anisotropic material [4]; this means there is no distinction between fibre and matrix inside. For the shell, the stress tensor has components ($\sigma_{11},\sigma_{22},\sigma_{12},\sigma_{23},\sigma_{13}$). The mechanical behaviour ply corresponds to damage-elasticity. Failure in the composite ply is introduced thanks to two variables d and d' whose values can grow from 0 (no damage) to 1 (total failure).

d' is linked to transverse crack in the matrix under tension, and is applied to transverse Young's modulus E_{22} by:

$E_{22}=E_{22}^0.(1-d')$ si $\sigma_{22} > 0$
$E_{22}=E_{22}^0$ si $\sigma_{22} < 0$ With E_{22}^0 initial modulus for undamaged ply.

d controls the shear cracks in fibre/matrix interface with the G_{12} shear modulus.

$G_{12}=G_{12}^0.(1-d)$
With G_{12}^0 representing initial shear modulus for undamaged ply.

Fibre fracture is given by the critical fracture strain of fibre ε_{11r}.

In this model, rising damage, which is given by d and d', intrinsically depends on internal strain energy within ply [5]. This notion of stored energy in the element is taken for the delamination model.

METHODOLOGY FOR THE DELAMINATION DETECTION AND FOLLOW-UP

Our methodology is based on the use and validation of post-process criteria of the explicit computational code. The criteria are applied on the interface using the stress tensor for each interface layer.

For the interface, the criteria are twofold:

The first is a strain energy density criterion, computed with the principal stresses $\sigma_1,\sigma_2,\sigma_3$, where E is Young's modulus, γ Poisson's ratio for the epoxy interface. This criterion Eqn 1 has all damage variables included in the effective stress.

$$\frac{dW}{dv} = \frac{1+\nu}{6E}.\left[(\sigma_1-\sigma_2)^2 + (\sigma_2-\sigma_3)^2 + (\sigma_3-\sigma_1)^2\right] + \frac{1-2\nu}{6E}(\sigma_1+\sigma_2+\sigma_3)^2 \qquad (1)$$

The second is the Tsai-Hill failure criterion (2). It is a quadratic stress criterion for ply. The ply is specified as an anisotropic material [6] and [7]. It uses the effective stress tensor as follows:

$$f^2 = \frac{\sigma_1^2}{X^2} + \frac{\sigma_2^2}{Y^2} - \frac{\sigma_{1*}\sigma_2}{X^2} + \frac{\tau_{12}^2}{U^2} + \frac{\tau_{23}^2}{S^2} + \frac{\tau_{31}^2}{S^2} \qquad (2).$$

X,Y,U and S are respectively longitudinal, transverse, and shear fracture threshold stress. For example, in this interface, X and Y are equal to 130 Mpa, U and S to 30 Mpa. f^2 value grow from 0 (no failure) to 1 (total failure).

Both criteria are used for delamination detection like filter factors at the interface of each element. An assessment of interfacial fracture can be given by a decrease in the energy density at interface, combined with a sufficiently high value of the Tsai-Hill criterion.

Damage variables are present in the computation due to the effective stress used in the criteria. We break down the problem into separate sequences of treatment :

- A first filter is applied onto the loading for delamination study. Threshold fracture limits for d and d' are selected (0.9 for our case). Data (stress, level of loading) relating to values lower than these damage values thresholds are kept to criteria treatment.

- For the element, evolution of energy density is computed. If it decreases more than 10% in terms of maximum energetic amplitude Fig. 2 then Tsai-Hill criterion is computed. If f^2 is bigger than 0.1, the energy dropping is taken like the failure level of loading. In the other case (no significant energy drop or f^2 less than 0.1) there is no failure and the energy density criterion computation is carried on.

- Corresponding failure loading and energy density reached are stored for each element. If the coupling criteria have not detected failure, critical loading values are those corresponding to damage values equal to 0.9.

It is important to consider these two criteria especially for meshing elements far away from the loading area. Actually, in these areas, energy density fluctuates around too low a value to characterize interface fracture. Therefore, Tsai-hill acts like a filter on low energy fluctuation.

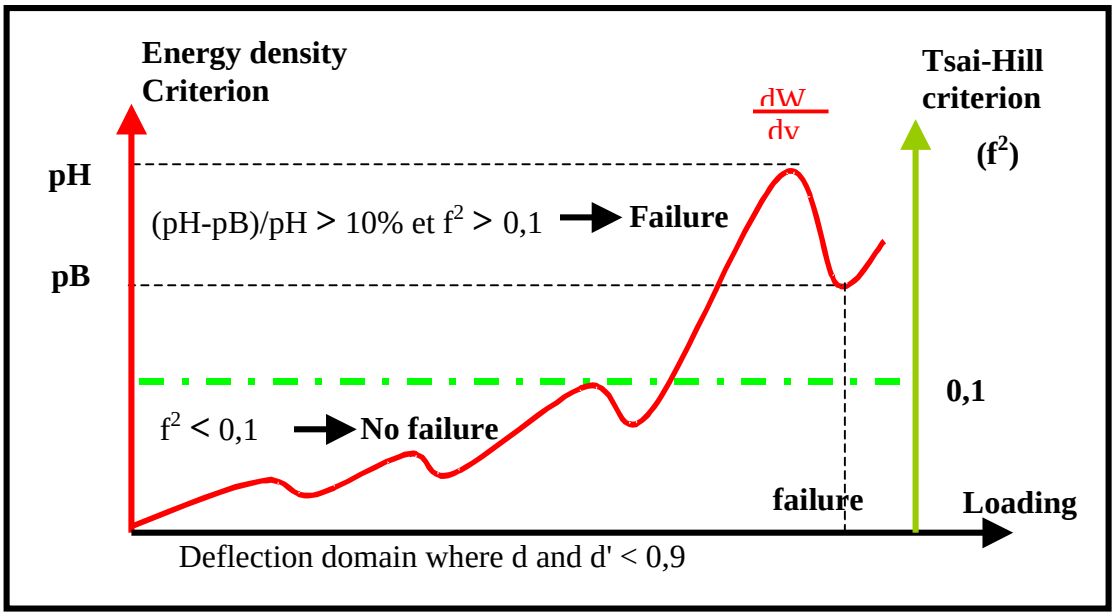

Fig. 2: Both criteria used for each interface element.

With the aim of having more accuracy in delamination study, a specific criterion for composite plies is added.

In fact, bottom interface 90/0 delamination of laminate $[90_2/0_2]_s$ is initiated by several transverse matrix cracks within the bottom 90° plies Fig. 3.

Cracks propagating in this 90° plies thickness appear from the bottom tensile plate's surface. When they reach 0° plies, they are deflected in the interface plane and start in several delamination fronts.
We apply a new criterion [8], which distinguishes tension Eqn 3 and compression Eqn 4 matrix failure.

Matrix failure in tension.:

$$\left(\frac{\sigma_{22}}{S_2}\right)^2 + \left(\frac{\sigma_{12}}{S_{12}}\right)^2 \geq 1 \qquad (3)$$

Matrix failure in compression.:

$$\left(\frac{\sigma_{22}}{2S_{12}}\right)^2 + \left[\left(\frac{C_2}{2S_{12}}\right)^2 - 1\right]\frac{\sigma_{22}}{C_2} + \left(\frac{\sigma_{12}}{S_{12}}\right)^2 \geq 1 \qquad (4)$$

Values taken for failure stress in transverse compression, shear and tensile transverse matrix are respectively: C_2 equal to 160 Mpa, S_{12} equal to 30 Mpa and S_2 equal to 35 Mpa.
So, in our case, for bottom 90° plies transverse cracks are generated by tension.

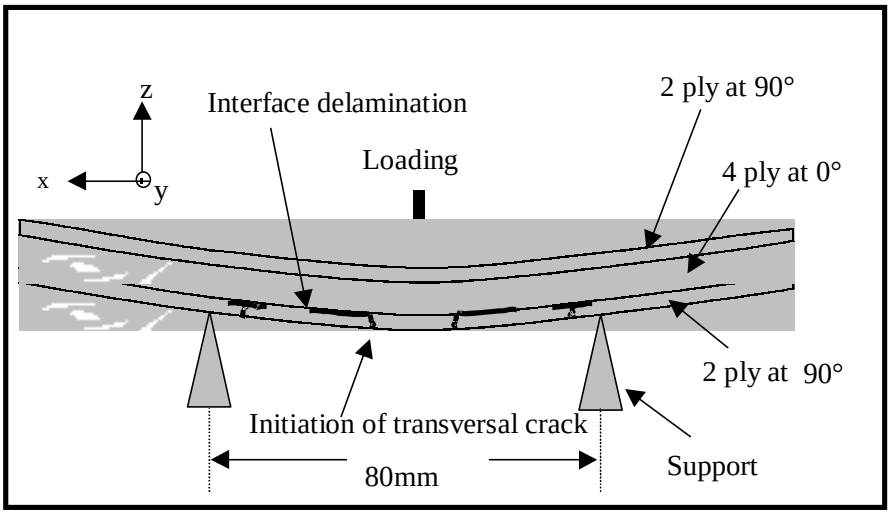

Fig. 3: Cross section of delamination growth for bottom interface 90/0.

DELAMINATION DETECTION

For the methodology validation, three nodes flexion plate on laminated composite has been selected.

Plate geometry is 200*50*4,9 mm^3. The bending is static for the experimental test (with 80 mm inter-support) and quasi-static in numerical code (1m/s for 15 Kg). This difference is due to the explicit code used.
Delamination growth is not a continuous function of deflection (displacement in the middle of the plate).

The Table 1 shows main deflection values corresponding to step of growth. It displays coherence between experimental and numerical.

Table 1: Comparison between critical growth deflections of delamination.

Test type	**Experimental**	**Numerical**	**% Error**
detection	Optical measurements	Criteria filtering	
Deflection 1	**2,63 mm**	**2,95 mm**	**10 %**
Deflection 2	**3,49 mm**	**3,89 mm**	**10 %**
Deflection 3	**4,51 mm**	**4,80 mm**	**6 %**
Deflection 4	**5,51 mm**	**5,68 mm**	**3 %**
Deflection 5	**6,52 mm**	**6,51 mm**	**0,2 %**
Deflection 6	**7,62 mm**	**7,29 mm**	**4,5 %**
Deflection 7	**8,52 mm**	**8,68 mm**	**1 %**
Deflection 8	**9,70 mm**	**9,80 mm**	**1 %**

Just as the transverse cracks in 90° ply, the Table 2 gives most cracks as a function of deflection level reach. A maximum error of 19% is displayed.

In numerical analysis for an element, we notice a potential 90° ply failure occurs before the delamination detection. So the chronology of damage mechanical appearance is in agreement with the experimental observation.

This chronological order is verified for deflection range comparison in tables 1 and 2.
Critical deflection steps for ply are lower than delamination deflection steps, and crack saturation happens before the end of the delamination growth.

Table 2: Comparison of deflection levels reach for 90° ply.

Test type	**Experimental**	**Numerical**	**% Error**
detection	90° ply optical measurements	Matrix criterion	
Deflection 1	**1,23 mm**	**0,99 mm**	**19 %**
Deflection 2	**1,90 mm**	**1,98 mm**	**4 %**
Deflection 3	**2,63 mm**	**2,95 mm**	**11 %**
Deflection 4	**3,49 mm**	**3,89 mm**	**11 %**
Deflection 5	**4,51 mm**	**4,80 mm**	**6 %**
Deflection 6	**5,84 mm**	**5,68 mm**	**2,73 %**

Differences between numerical and experimental may be justified for this model by growth of crack dependence with mesh length. That explains an inaccuracy, especially for the low deflection level, when the ply crack is smaller than shell length.

INTERGRATION OF DELAMINATION EFFECTS

To evaluate in the finite element code the effects of the delamination displayed using the criteria, two simulation types are made:

- "Sequential" computation, which integrates delamination effects within laminated plate. Those effects over modelling are included in code by weakening the mechanical features of the sublaminate plies at delaminated interface. Thus, the influence of those plies over the overall structure stiffness is limited. This weakness has a progressive distribution inside the plate as a function of the delaminated matrix failure element location in the model.
- "direct" computation, without any integration of the delamination effect. There are no modifications of the mechanical features during loading.

Fig 4 displays some integrated damage distribution in a quarter bending plate model due to sequential computation. In the model, delamination is associated with damage values close to 1. We must notice that d and d' for interface are given with the same evolution law.

On the one hand, we notice a transverse crack in the bottom 90° ply for 1.98 mm of deflection. On the other hand, the first transverse delamination strip is detected at 2.96 mm of deflection within interface. So, the mechanical damage for sequential computation is in agreement with the experimental chronology

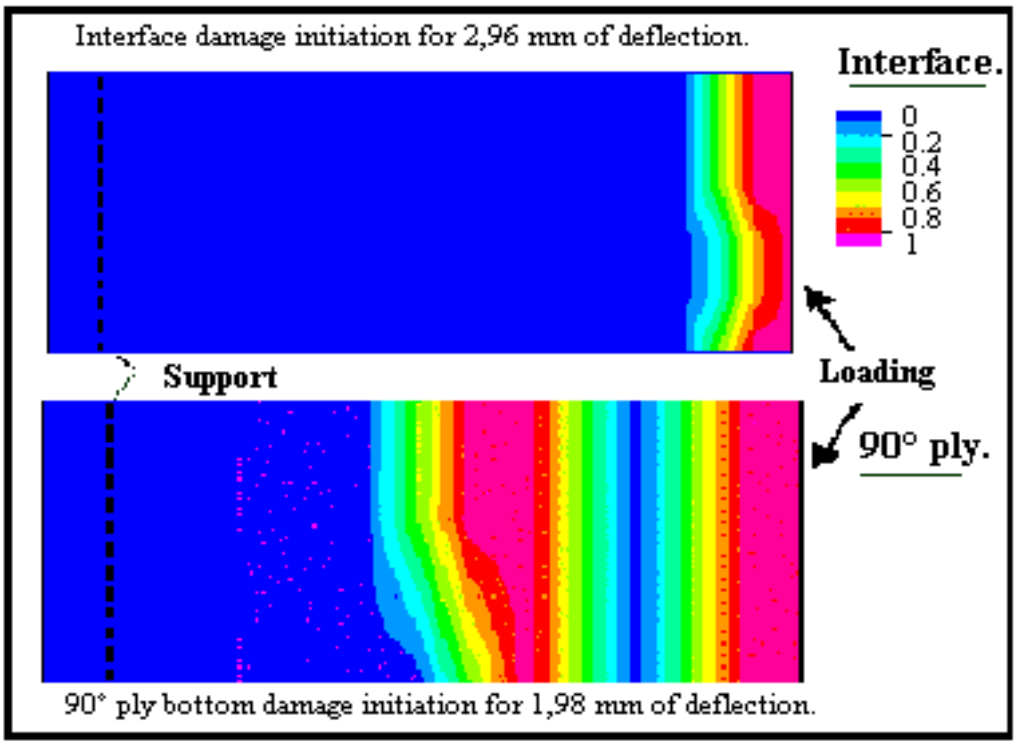

Fig. 4: Damage initiation in sequential computation for quarter-plate.

Concerning delamination growth during the process, Fig. 5 and Fig. 6 give an example of delamination distribution for experimental test. This ultrasound sweep report is carried out for a given deflection. It shows discontinuous transverse strips like the observation taken for this configuration in bibliography [9].

A quarter plate equivalent model is compared with experiments. The sequential computation gives a similar distribution of delamination. This restitution is not found in direct computation where delamination is only like a single transverse delamination front reaching from the middle of the plate to the edge.
The delamination distribution accuracy depends of meshing: minimum step of delamination growth is directly linked to the shell length.

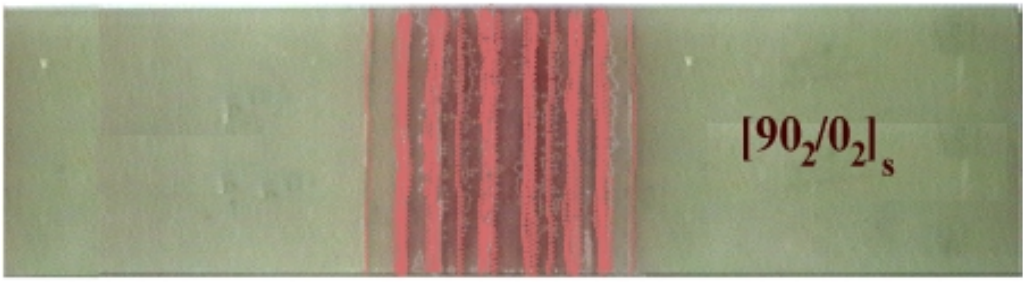

Fig. 5: Strips delamination visible on bottom surface laminated plate.

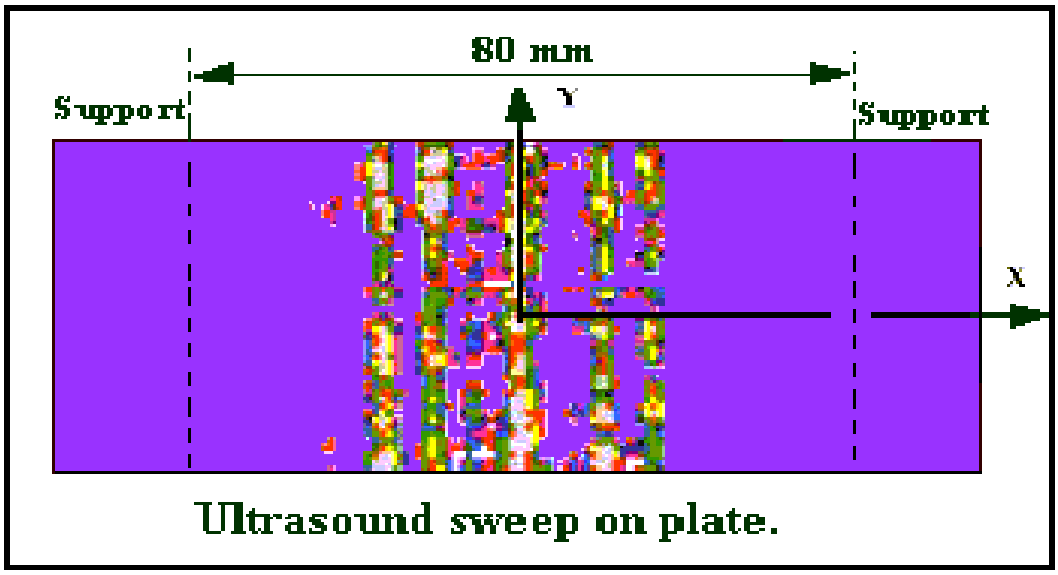

Fig. 6: Ultrasound sweep delamination localisation in interface.

QUANTITATIVE ANALYSIS OF NUMERICAL DELAMINATION EFFECTS

This analysis is based on strain energy growth during loading. This evolution is displayed by Fig. 7 as a function of displacement, for the two computational types and the static experiment-bending test.

The energetic evolution experiments is estimated thanks to strain gauges on top and bottom surfaces plate. The strain curves give energy strain density estimate within the plate.

For the sequential computation, loading reached and failure deflection (14mm) are more coherent with experiments than "direct" computation which overrates these values.

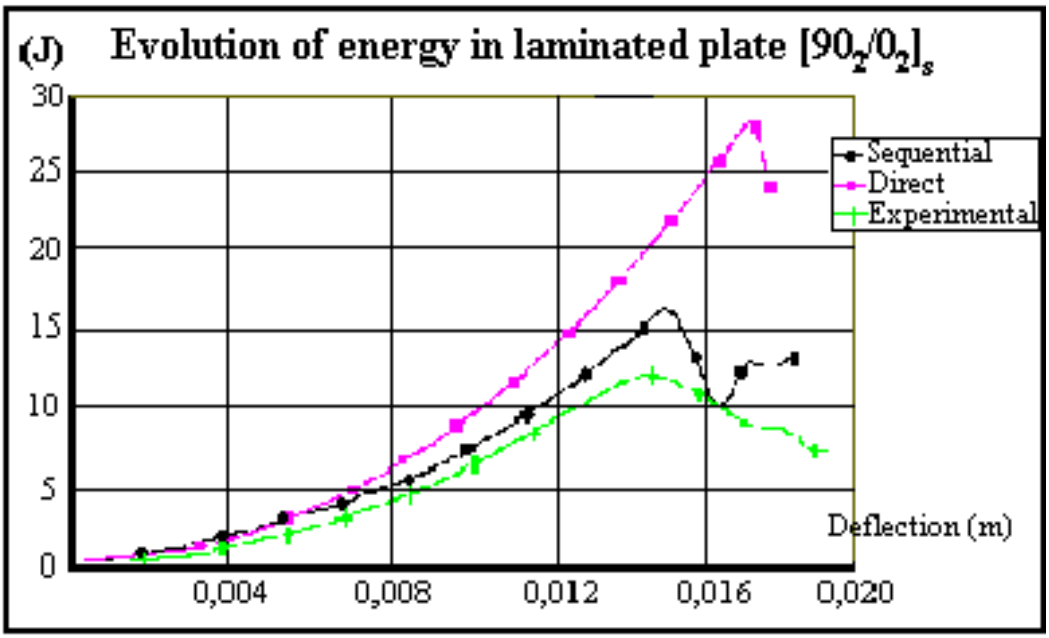

Fig. 7: Comparison of energetic evolutions between numerical and experimental.

CONCLUSIONS

A methodology is suggested for the delamination study and the restitution of mechanical effects in multi-layered shell element. Energetic and stress criteria are applied in post-treatment of an explicit finite-elements code. It was able to follow both the initiation and the delamination growths. Progressive integration of damage in the model gives a better accuracy of the failure levels reached (in loading and displacement) with an experimental validation test.

However, an accurate delamination detection is linked with meshing. The propagation length cannot be smaller than the mesh. Arrangement must be found for the given model. Furthermore, if this methodology is applied to shells, all fracture modes can not be taken in account.

The purpose of this development process in explicit code is the laminated structure crash study. We put the emphasis on the importance of suitable interface models.

Experimental tensile test will be achieved to characterize interface damage, and dynamic validation will be carried out.

ACKNOWLEDGEMENTS

The authors would like to acknowledge the supports of the CNRS, Région Nord Pas de Calais and the ONERA.

REFERENCES

1. O'Brien, T.K., "Characterization of delamination onset and growth in a composite laminate.", Damage in Composite Materials, ASTM STP 775, K.L. Reifsnider,Ed., Amarican society for testing and Materials, 1982, pp.140-167.

2. Allix, O. and Ladevèze, P., "Damage analysis of interlaminar fracture specimens.", Journal of Composite Materials, Vol.31, 1995, pp. 61-74.

3. Sun, C.T. and Manoharan, M.G., " Growth of delamination cracks due to bending in a $[90_5/0_5/90_5]$ laminate.", Composites Science and Technology, Vol.34, 1989, pp. 365-377.

4. Coutellier, D., Gauthier, C., Rozycki, P. and Ravalard, Y., "Numerical simulation of tensile behaviour of multilayered multilayered multi-materials within an explicit software code.", European Journal of Mechanicals Environmental Engineering,Vol.43, No. 2, 1998, pp.51-60.

5. Usik. Lee., Lesieutre,G.A. and Lei. Fang., "Anisotropic damage mechanics Based on strain enregy equivalence and equivalent elliptical microcracks.", International Journal of Solids Structures, Vol.34, No. 33, 1997, pp. 4377-4397.

6. Brewer, J.C. and Lagace, P.A., "Quadratic stress criterion for initiation of delamination.", Journal of Composite Materials, Vol.22, 1988, pp.1141-1155.

7. Tsai, W.S. and Wu, E.M., "A general theory of strength for anisotropic materials.", Journal of Composite Materials, Vol.5, 1971, pp58-80.

8. Choi, H.Y., and Chang, F.K., "A model for predicting damage in graphite/Epoxy laminated composites resulting from low-velocity point impact.", Journal of Composite Materials, Vo26, No14, 1992, pp. 2134-2168.

9. Hyung. Yun. Choi. and Fu-Kuo. Chang., "A model for predicting damage in Graphite/Epoxy laminated composites resulting from low-velocity point impact.", Journal of Composite Materials, Vol.26, No. 14, 1992, pp.2134-2168.